Sitespecific fragmentation in condensed (CH3S)2 by sulfur Kedge photoexcitation

Y. Baba, K. Yoshii, and T. A. Sasaki

Citation: The Journal of Chemical Physics **105**, 8858 (1996); doi: 10.1063/1.472615
View online: http://dx.doi.org/10.1063/1.472615
View Table of Contents: http://scitation.aip.org/content/aip/journal/jcp/105/19?ver=pdfcov
Published by the AIP Publishing

Site-specific fragmentation in condensed $(CH_3S)_2$ by sulfur *K*-edge photoexcitation

Y. Baba,[a] K. Yoshii, and T. A. Sasaki
Advanced Science Research Center, Japan Atomic Energy Research Institute, Tokai-mura, Naka-gun, Ibaraki-ken, 319-11, Japan

(Received 15 April 1996; accepted 12 August 1996)

The site-specific fragmentation by core-to-valence resonant photoexcitation has been investigated for condensed $(CH_3S)_2$ (dimethyl disulfide). The data presented are the desorption yields of the fragment ions from multilayered $(CH_3S)_2$ around the sulfur *K*-edge photoexcitation as well as the x-ray absorption and Auger decay spectra. The x-ray absorption spectrum exhibits the double structure of the S $1s\rightarrow\sigma^*$ resonance peak corresponding to the S $1s\rightarrow\sigma^*$(S–S) and S $1s\rightarrow\sigma^*$(S–C) photoexcitations. It was found that the S $1s\rightarrow\sigma^*$(S–C) excitation is predominantly followed by the CH_3^+ desorption, but the CH_3^+ and S^+ ions are desorbed in comparable intensity at the S $1s\rightarrow\sigma^*$(S–S) excitation. The Auger decay spectra around the S $1s\rightarrow\sigma^*$ excitation revealed that there exist two kinds of sulfur $KL_{2,3}L_{2,3}$ spectator Auger decay originating from the S $1s\rightarrow\sigma^*$(S–S) and S $1s\rightarrow\sigma^*$(S–C) resonant excitations. The observed site-specific fragmentation is interpreted in terms of the localization of the spectator electron in each antibonding orbital, i.e., σ^*(S–S) and σ^*(S–C). © *1996 American Institute of Physics.* [S0021-9606(96)00443-6]

I. INTRODUCTION

Photochemical reaction at solid surfaces has been extensively investigated in the fields of catalysis, biochemistry, semiconductor processing, and so forth. Generally, the energy of photons used in surface photochemistry are visible and ultraviolet region for the purpose of exciting or ionizing valence electrons in molecules. On the other hand, the energy of x ray is so high that the irradiation of x rays on a molecule would excite or ionize the inner-shell electrons which do not participate in the chemical reaction. Therefore, it is natural that one might imagine that x ray is not suitable for the control of photochemical reactions. Actually a molecule irradiated by x ray tends to be randomly broken up, and such a process is one of the main subjects in the field of radiation chemistry and radiation biology.

However, recent popularization of energy-tunable and highly polarized synchrotron radiation has opened a possibility that soft x rays (~0.1–10 keV) could be used as incident photons in surface photochemical reaction. We consider that there are mainly two advantages in using synchrotron soft x-rays as incident photons in surface photochemistry. The first is the ''element selectivity'' and the second is the ''site selectivity'' of primary photoexcitation.

The element selectivity is based on the fact that the energy of core levels is inherent to the element. This means that the core electron of a specific element in a molecule can be excited or ionized by tuning the energy of x rays. The examples of the element selectivity of core excitation have been reported concerning the fragmentation in solid NO and CO,[1] and NO[2] adsorbed on Ru(001) following the *K*-edge photoexcitation. The present authors have also reported the examples of the element-selective ion desorption from solid $SiCl_4$,[3,4] PCl_3,[5] and S_2Cl_2 (Ref. 6) following the photoexcitations at the *K* edges.

The site selectivity is based on the fact that the core-to-valence photoexcitation is primarily localized in a specific chemical bond. If the primary excitation around a specific chemical bond is still localized at the site until the chemical-bond breaking happens, the site-specific chemical reaction is realized. Actually the site-specific fragmentation by inner-shell photoexcitation has been observed in adsorbed molecules[7–10] and bulk materials.[11,12] The explicit example of the site selectivity has been demonstrated by Tinone *et al.*[11,12] who observed the different fragmentation patterns depending on the photon energy in polymer thin films (PMMA) by carbon and oxygen *K*-edge photoexcitations.

The examples of such site-specific fragmentation by inner-shell photoexcitation have rather been extensively investigated in gas-phase molecules.[13–24] In comparison with gas-phase molecules, the mechanism of the site-specific photochemical reaction at solid surfaces is still open owing to the complexity of the decay dynamics in solid or its surface. The main origins of the complexities of the decay dynamics in solid or its surface are; (i) effect of the inelastically scattered electrons on the fragmentation, (ii) screening effect by adjacent atoms on the decay processes, and (iii) structural factors such as crystal structure of solid and molecular orientation of adsorbates. In order to clarify the mechanism of the site-specific photofragmentation and desorption at solid surface, we consider that it is essential to investigate the total deexcitation processes including Auger decay (fluorescent x-ray emission) and fragmentation in the same adsorbed system.

In the present paper, we present a site-selective fragmentation in an adsorbed simple molecule following the core-to-valence photoexcitation as well as the x-ray absorption and Auger decay spectra. Here we investigate the desorption of

[a]Author to whom correspondence should be addressed.

fragment ions from multilayered $(CH_3S)_2$ (dimethyl disulfide, DMDS) following the S $1s\rightarrow\sigma^*$ resonant-photoexcitation. The structure of DMDS is CH_3–S–S–CH_3 (C_2 symmetry) with C–S–S bond angle of about 140°. This molecule is an appropriate example to investigate the site-selective fragmentation by core-to-valence resonant photoexcitation, because the sulfur atom of this molecule is coordinated to two kinds of different atoms, i.e., sulfur and carbon. Also, DMDS is the simplest prototype of amino acid containing S–S bond such as cystine, and the primary process of the x-ray-induced fragmentation of this molecule is quite important in the fields of radiation biology and radiation chemistry.

II. EXPERIMENT

The experiments were performed at the BL-27A station of the Photon Factory in the National Laboratory for High Energy Physics (KEK-PF) employing double crystal of InSb(111) plane as a monochromator. The energy resolution of the monochromator was 1.2 eV at 2.5 keV.

The details of the experimental apparatus and procedures were almost the same as those described elsewhere.[3] The followings are the brief outline of the experimental setups. High-purity solution of DMDS was purified through several freeze–pump–thaw cycles, and dosed onto the clean surface of Cu(100) at 85 K through a gas doser made of glass filter. The thickness of the adsorbate, determined by the temperature-programmed desorption (TPD) measurements, was 300 layers. The x-ray absorption near edge structures (XANES's) were measured by a total electron yield (TEY) obtained by the sample current.

The desorbed ions were measured by a quadrupole mass spectrometer (ULVAC QMS-1000) operating in a pulse-counting mode. The vacuum pressure during the desorption measurements was kept less than 2×10^{-8} Pa. Two mesh grids were located between sample and mass spectrometer. The first grid (G_1) was grounded, and the second one (G_2) was negatively biased at -30 V to extract positive ions. The sample was floated at $+40$ V during the measurements. The polar angle of the electric vector of the incident x-rays was 7° and the takeoff direction of the ions was 83° from the surface.

The Auger decay spectra were measured by a hemispherical electron energy analyzer (VSW. CLASS-100). The polar angle of the electric vector of the incident x rays was 35° and the takeoff direction of the Auger electrons was surface normal. Both electron and ion yields were normalized by the photon intensity measured by the current of copper mesh located in front of the sample.

III. RESULTS

A. XANES spectra

XANES spectrum taken by the total electron yield mode for multilayered DMDS is displayed in Fig. 1 as topmost spectrum (solid line). The number indicated in the electron yield curve represents the photon energy used for the measurements of the Auger decay spectra (Fig. 4). The sharp resonance peak with double structure (marked A) and broad one (marked B) are observed in this energy region. In comparison with many of the gas-phase XANES spectra for alkylated divalent sulfur compounds,[25–27] the first intense peak A can be assigned as the S $1s\rightarrow\sigma^*$ (S $3p^*$) excitation and the second broad peak B is ascribed to the shape resonance corresponding to the excitation into higher unoccupied orbitals such as S $3d^*$ and S $5s^*$. It is noticeable that the peak A is split into two components.

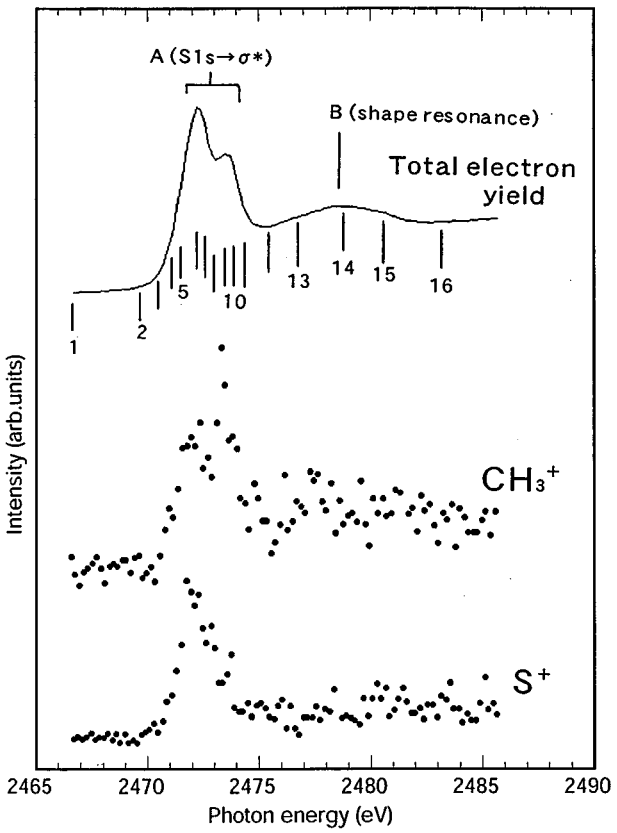

FIG. 1. Photon energy dependences of total electron yield (solid line) and ion desorption yield (dotted lines) for multilayered DMDS around the sulfur K-edge excitation. Total electron yield curve corresponds to the x-ray absorption spectrum (XANES). The number indicated in the total electron yield curve represents the photon energy used for the measurements of the Auger decay spectra (Fig. 4).

Figure 2 is the same spectrum but in an expanded energy scale. The energy separation of the two components is 1.2 eV. Such peak splitting in the S $1s\rightarrow\sigma^*$ is never seen in divalent sulfur compounds containing a single S atom, such as dimethyl sulfide.[27] The occupied valence shell of the ground state of DMDS is $(9a)^2(10a)^2(9b)^2(10b)^2(11b)^2(11a)^2(12a)^2(13a)^2(12b)^2$.[28] The outermost $12b$ and $13a$ orbitals are almost nonbonding and their main components are S $3p$ orbitals.[29] The $12a$ orbital consists of σ (S–S) and $11a$ and $11b$ orbitals have σ (S–C) character.[29] The energy levels of the σ (S–S) and σ (S–C) orbitals for gas-phase DMDS have been measured by ultraviolet photoelectron spectroscopy (UPS).[28,30] The energy separation between

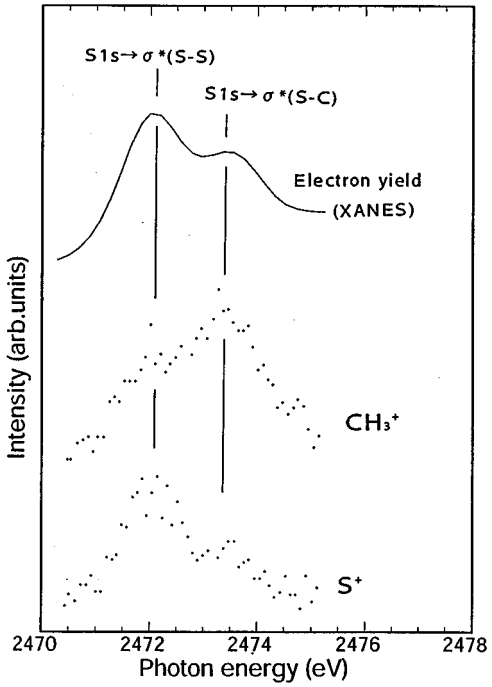

FIG. 2. Same as Fig. 1 but in an expanded energy scale around the S $1s\rightarrow\sigma^*$ resonance.

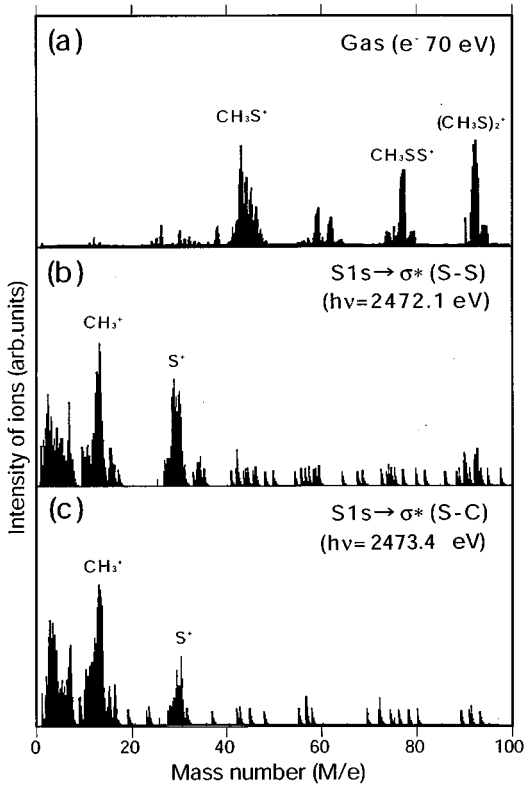

FIG. 3. Mass spectra of fragment ions for DMDS. The topmost spectrum (a) represents the fragment ions of gas-phase DMDS molecule irradiated by 70 eV electrons (so-called cracking pattern). The middle (b) and the lowest (c) spectra show the desorbed ions from multilayered DMDS at the photon energies of the S $1s\rightarrow\sigma^*$(S–S) and S $1s\rightarrow\sigma^*$(S–C) resonances, respectively.

11*a* and 12*a* orbitals in UPS spectrum is close to the present value of the energy splitting of the S $1s\rightarrow\sigma^*$ peak. It has been established that the relative energy levels of molecular orbitals scarcely change from gas phase to van der Waals molecular condensate. This is indeed the case for the DMDS adsorbed on Cu(111) surface at various temperatures.[30] Considering a mirrorlike structure between occupied and unoccupied levels in valence region, we assign the lower- and higher-energy components as the excitations from S 1*s* to the σ^*(S–S) and σ^*(S–C), respectively. This is consistent with the simple assignment of the XANES spectrum of gas-phase DMDS by Hitchcock *et al.*[31] Similar energy splittings in the S $1s\rightarrow\sigma^*$ resonance peaks were also observed in condensed layers of the S–S containing compounds such as dichlorodisulfide (Cl–S–S–Cl)[32] and dibutyldisulfide $(C_4H_9–S–S–C_4H_9)$.[33]

B. Ion desorption

Figure 3 displays mass spectra of fragment ions for DMDS. The topmost spectrum (a) represents the fragment ions of gas-phase DMDS irradiated by 70 eV electrons (so-called cracking pattern of quadrupole mass spectrometer). The middle (b) and the lowest (c) spectra show the desorbed ions at the photon energies of the S $1s\rightarrow\sigma^*$(S–S) and S $1s\rightarrow\sigma^*$(S–C) resonances, respectively. The resolutions of these two spectra are a little reduced in comparison with that of the gas-phase spectrum to get a high detection efficiency. The gas-phase spectrum exhibits parent ions $[(CH_3S)_2^+]$ and some molecular fragments (CH_3S^+, $CH_3S_2^+$, etc.). On the other hand, only S^+ and CH_3^+ ions (and some doubly charged species of low mass number) are seen in the desorption spectra. The appreciable difference between gas-phase spectrum and photon-stimulated desorption spectra suggests that the desorption of the ions is triggered not by a secondary effect such as excitation by inelastically scattered low-energy electrons but directly by primary core-to-valence photoexcitation.

The photon-energy dependences of the S^+- and CH_3^+-ion yields are presented in Fig. 1 as dotted curves. Also they are shown in Fig. 2 in an expanded energy scale. Two different features are seen between electron-yield and desorption-yield curves. First, the excitation at the shape resonance (peak B in Fig. 1) yields scarcely any ion desorption. Secondly, the S^+ ions are desorbed mainly at the S $1s\rightarrow\sigma^*$(S–S) resonance while the CH_3^+ ions are desorbed predominantly at the S $1s\rightarrow\sigma^*$(S–C) excitation (Fig. 2). The latter feature is quite interesting because the site-specific desorption apparently happens by the photoexcitation from the same core orbital to the different unoccupied valence orbital. If the excited electrons are localized at the respective chemical bonds until the fragmentation happens, the observed tendency that the S $1s\rightarrow\sigma^*$(S–S) resonance yields S^+ desorption and S $1s\rightarrow\sigma^*$(S–C) resonance induces CH_3^+ desorption is quite natural because both of the σ^* orbitals are strongly antibonding. The localized nature of the primary photoexcitations will

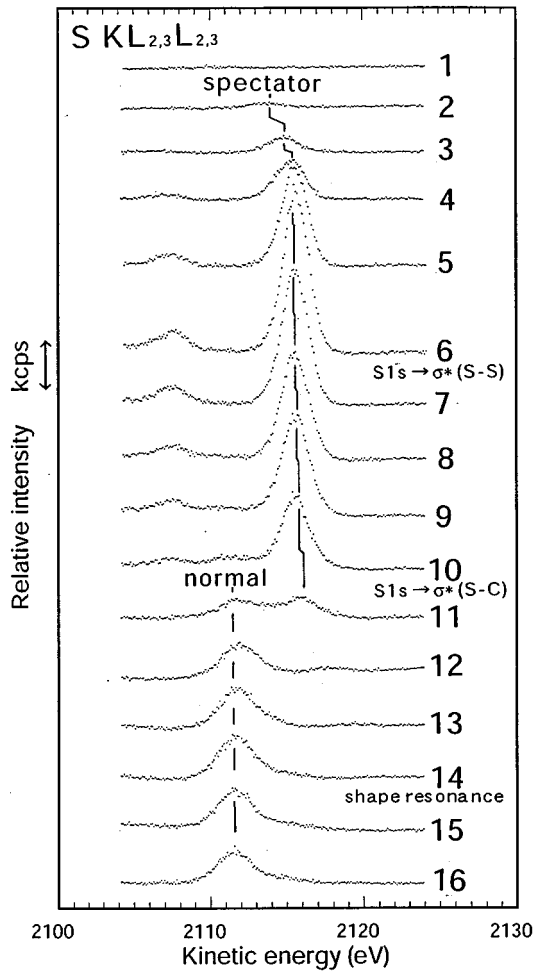

FIG. 4. Auger decay spectra of multilayered DMDS in sulfur $KL_{2,3}L_{2,3}$ region excited by various photon energies around the sulfur K-edge. The number indicated in each spectrum corresponds to the photon energy shown in the total electron yield curve in Fig. 1.

be discussed on the basis of the Auger decay spectra in the next section.

C. Auger decay

When a core-electron is resonantly excited into one of the valence unoccupied orbitals, a resonant Auger-decay is the main primary deexcitation channels in a light element like sulfur (fluorescent x-ray emission is about 6% of the total deexcitation process in sulfur[34] so that it is not considered here). It has been established that the resonantly excited neutral states is followed by two types of Auger decays, i.e., spectator and participator Auger decays.[35] The details of these two decay channels initiated by the $1s\rightarrow 3p^*$ resonant excitation have been described elsewhere concerning the similar materials.[4,36–41] In the present case, the most intense Auger lines after the S $1s\rightarrow\sigma^*$ excitation would be sulfur $KL_{2,3}L_{2,3}$ spectator Auger lines and sulfur $KL_{2,3}$ participator Auger line. The former appears near the sulfur $KL_{2,3}L_{2,3}$ normal Auger line and the latter is observed as the enhancement of the sulfur $L_{2,3}$ (S $2p$) photoelectron.[39]

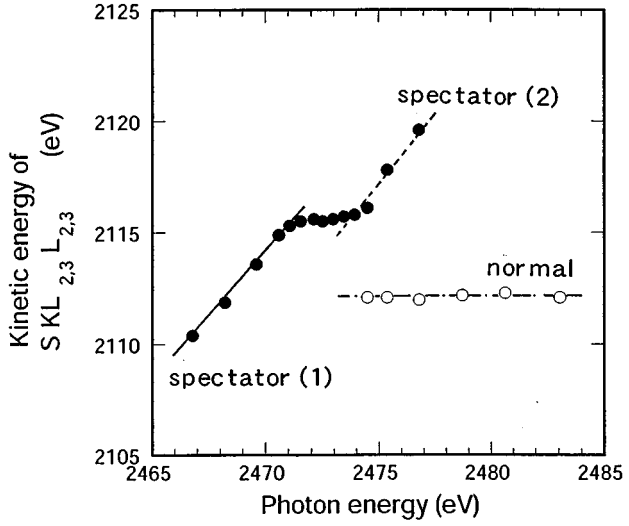

FIG. 5. Relation between incident photon energy and the kinetic energy of the sulfur $KL_{2,3}L_{2,3}$ Auger line for multilayered DMDS around the sulfur K-edge excitation.

The Auger-decay spectra around the sulfur $KL_{2,3}L_{2,3}$ region taken at various photon energies around the S $1s\rightarrow\sigma^*$ resonance are shown in Fig. 4. The number indicated in each spectrum corresponds to the photon energy shown in the electron-yield curve in Fig. 1. The normal Auger peak with fixed kinetic energy apparently begins to appear from spectrum 11. The higher kinetic-energy peaks observed in the spectra 2–11 originate from the spectator Auger decay. Concerning the energy of the $KL_{2,3}L_{2,3}$ spectator Auger electrons, we have observed the linear dispersion with the incident photon energy for condensed molecules such as $SiCl_4$ (Refs. 40 and 41) and CS_2 (Refs. 38 and 41) around the $1s\rightarrow\sigma^*(3p^*)$ resonances. This phenomenon is ascribed to the Auger resonant Raman effect. Similar kinetic-energy shift with the photon energy is also observed for this higher-energy peak.

In Fig. 5 the kinetic energies of the sulfur $KL_{2,3}L_{2,3}$ Auger peaks are plotted as a function of incident photon energy. A two-step linear kinetic-energy dispersion is clearly observed in the spectator Auger peaks. Similar two-step linear dispersion was also observed in $SiCl_4$ around the Cl $1s\rightarrow\sigma^*$ excitation where the Cl $1s\rightarrow\sigma^*$ resonance peak in XANES spectrum has similar kind of double structure.[41] Such two-step linear dispersion was explained by a fact that two kinds of the resonant excitations induce respective Auger resonant Raman effect.[41] When the photon energy regions of linear dispersions are compared with those of the double structures in XANES spectrum (Fig. 2), the first linear line marked as spectator (1) corresponds to the sulfur $KL_{2,3}L_{2,3}$ spectator Auger peak following the S $1s\rightarrow\sigma^*$ (S–S) excitation, and the second one marked as spectator (2) originates from that following the S $1s\rightarrow\sigma^*$ (S–C) excitation. Therefore, it is important that both the S $1s\rightarrow\sigma^*$ (S–S) and S $1s\rightarrow\sigma^*$ (S–C) excitations are primarily followed by the respective spectator Auger decays. This finding suggests that the ex-

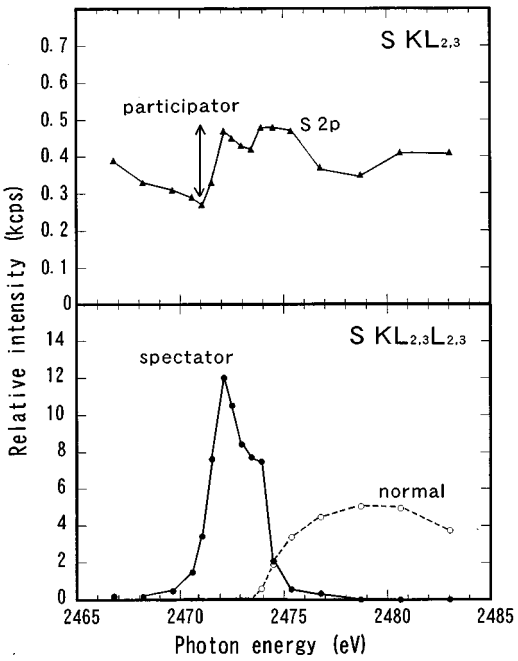

FIG. 6. Intensities of the sulfur $KL_{2,3}L_{2,3}$ Auger peak and sulfur $KL_{2,3}$ participator Auger peak as a function of incident photon energy. The contribution of the sulfur $KL_{2,3}$ participator Auger decay corresponds to the enhancement of the S $2p$ photoelectron peak at the resonant excitation (indicated as arrow).

cited electrons (hereafter, we call this electron as a ''spectator electron'') are localized at the respective chemical bonds in the course of the Auger decay.

Figure 6 summarizes the photon-energy dependences of the peak intensities of various Auger lines. We have measured the other possible primary decay channels such as sulfur $KL_1L_{2,3}$, KL_1L_1, $KL_{2,3}V$, and KL_1V spectator decays and sulfur KL_1 participator decays, but it was turned out that the contributions of these decay channels are less than ~10% of the $KL_{2,3}L_{2,3}$ decay. When we compare Fig. 6 with the XANES spectrum in Fig. 1, it is revealed that the S $1s\rightarrow\sigma^*$ resonant excitation is mostly followed by the sulfur $KL_{2,3}L_{2,3}$ spectator Auger decay but the participator decay channels play a minor role. Also it is seen that the shape resonance is virtually followed by the sulfur $KL_{2,3}L_{2,3}$ normal Auger decay.

IV. DISCUSSION

Before the discussion about the desorption mechanism, the main three points of the results will be briefly reviewed as follows:

(1) The XANES spectrum around the sulfur K edge exhibits a sharp peak of the S $1s\rightarrow\sigma^*$ resonance with double structure [S $1s\rightarrow\sigma^*$ (S–S) and S $1s\rightarrow\sigma^*$ (S–C)] and a broad peak of the shape resonance. The S^+ ions are mainly desorbed at the S $1s\rightarrow\sigma^*$ (S–S) resonance and the S $1s\rightarrow\sigma^*$ (S–C) resonance predominantly yields the CH_3^+ desorption. The shape resonance results in scarcely any ion desorption.

(2) The main-decay channel after the S $1s\rightarrow\sigma^*$ resonance is the sulfur $KL_{2,3}L_{2,3}$ spectator Auger decay, but the shape resonance is followed only by the sulfur $KL_{2,3}L_{2,3}$ normal Auger decay.

(3) The sulfur $KL_{2,3}L_{2,3}$ spectator Auger peak is composed of two components corresponding to the spectator decays following the S $1s\rightarrow\sigma^*$ (S–S) and S $1s\rightarrow\sigma^*$ (S–C) resonances. This fact suggests the spectator electron is localized in each chemical bond during the Auger decay.

The main decay channels and possible sequences of the electronic configurations are summarized in Table I concerning the four primary excitation modes, i.e., S $1s\rightarrow\sigma^*$ (S–S) resonance, S $1s\rightarrow\sigma^*$ (S–C) resonance, shape resonance and S $1s$ ionization. In this table, σ^{*1} represents the spectator electron and v denotes the valence orbital. The positive and negative indices marked in the orbital show the number of electron and holes, respectively. The primary $KL_{2,3}L_{2,3}$ transitions are followed by the $L_{2,3}VV$ Auger decays where V represents the valence orbital. In the previous paper, we have reported that the $2p^{-2}\sigma^{*1}$ state created by the $KL_{2,3}L_{2,3}$ spectator Auger decay in a similar molecule is followed by the initial $L_{2,3}VV$ Auger decay with one $2p$ hole which yields two valence holes, and succeeding $L_{2,3}VV$ decay without $2p$ hole which yields four valence holes.[39] Although we could not distinguish between spectator and normal Auger decays in $L_{2,3}VV$ Auger decay spectra due to the broad peak structures, we tentatively assign that the spectator Auger decay would be predominant by taking the KLL results into consideration. Thus the final electronic configuration at the S $1s\rightarrow\sigma^*$ resonance is shown as $v^{-4}\sigma^{*1}$ in Table I.

It has been established that the positive-ion desorption

TABLE I. The main decay channels and possible sequences of the electronic configurations. v represents one of the valence orbitals, and the index shown in each orbital denotes the number of electrons. $\sigma_{S-S}{}^{*1}$ and $\sigma_{S-C}{}^{*1}$ are the spectator electrons localized in the S–S and S–C bonds, respectively.

Excitation mode	Electronic configuration	Desorption
S$1s\rightarrow\sigma_{S-S}{}^*$	$[1s^{-1}\sigma_{S-S}{}^{*1}] \xrightarrow[KL_{2,3}L_{2,3}\text{ (spec.)}]{} [2p^{-2}\sigma_{S-S}{}^{*1}] \xrightarrow[L_{2,3}VV]{} [2p^{-1}v^{-2}\sigma_{S-S}{}^{*1}] \xrightarrow[L_{2,3}VV]{} [v^{-4}\sigma_{S-S}{}^{*1}]$	$\rightarrow S^+, CH_3^+$
S$1s\rightarrow\sigma_{S-C}{}^*$	$[1s^{-1}\sigma_{S-C}{}^{*1}] \xrightarrow[KL_{2,3}L_{2,3}\text{ (spec.)}]{} [2p^{-2}\sigma_{S-C}{}^{*1}] \xrightarrow[L_{2,3}VV]{} [2p^{-1}v^{-2}\sigma_{S-C}{}^{*1}] \xrightarrow[L_{2,3}VV]{} [v^{-4}\sigma_{S-C}{}^{*1}]$	$\rightarrow$mostly CH_3^+
S$1s\rightarrow 3d^*(5s^*)$ (shape resonance)	$[1s^{-1}3d^{*1}] \xrightarrow[KL_{2,3}L_{2,3}\text{ (norm.)}]{} [2p^{-2}] \xrightarrow[L_{2,3}VV]{} [2p^{-1}v^{-2}] \xrightarrow[L_{2,3}VV]{} [v^{-4}]$	$\rightarrow$few
S$1s\rightarrow$ionization	$[1s^{-1}] \xrightarrow[KL_{2,3}L_{2,3}\text{ (norm.)}]{} [2p^{-2}] \xrightarrow[L_{2,3}VV]{} [2p^{-1}v^{-2}] \xrightarrow[L_{2,3}VV]{} [v^{-4}]$	$\rightarrow$few

following inner-shell ionization is in many cases well explained on the basis of the localization of two or more positive holes in valence orbitals which are created by the sequence of the Auger decays (KF model).[42] The Coulomb interaction between the two holes in an Auger final state leads to the localization of this state if the Coulomb energy is larger than the band width of the corresponding hole state, and finally resulting in the fragmentation and desorption due to the Coulomb repulsion.[43] This scenario is indeed the case for the adsorbed molecules (condensate) with relatively narrow band width of one-hole state,[43] except for monolayered adsorbates on metal substrate where the valence holes are well screened by the electrons in metal substrate.[44,45] Also in the present case, the KF process would be predominant in the photon energy range where the normal Auger decay happens. On the other hand, at the core-to-valence resonant excitation where the spectator Auger decay happens, the effect of the remaining electron in the σ^* orbital on the desorption process must be also taken into account. If the KF model can be applied not only to the core ionization but also to the resonant core excitation, the photon-energy dependence curve of the ion desorption yield would be identical to that of the total electron yield, because the total electrons are mostly composed of inelastically scattered low-energy electrons irrespective of the primary Auger decay processes. However this is not the case for the present results (Fig. 2). Therefore, the observed dissimilarity between the XANES and ion yield suggests that there exist the other process than the KF process in the S^+ and CH_3^+ desorption.

The first point of the dissimilarity is the disappearance of the shape resonance peak in the desorption-yield curves (Fig. 1). This result implies that the desorption of some fragment ion is enhanced by a special core-to-valence photoexcitation mode. Similar results have been reported for condensed H_2O,[7] NH_3,[44] and benzene[46] at the *K*-edge photoexcitation. Also the present authors have observed the enhancement of the Cl^+ desorption from multilayered CCl_4,[47] $SiCl_4$,[3,4] and PCl_3 (Ref. 5) at the Cl *K*-edge excitation, where the Cl $1s\rightarrow\sigma^*$ resonant excitation yields Cl^+ desorption but higher-energy resonances such as Cl $1s\rightarrow 3d^*$ and $5s^*$ do not induce scarcely any Cl^+ desorption. In both sulfur and chlorine cases, the primary decay channels at the higher-energy resonances are completely $KL_{2,3}L_{2,3}$ normal Auger decay. This fact implies that the final electronic configuration like v^{-4} does not so much contribute to the fragmentation and ion desorption. Namely the spectator electron in the σ^* orbital is essential for the fragmentation.

The second point of the dissimilarity between electron and ion yield curves is the intensity ratio of the S $1s\rightarrow\sigma^*$ (S–S) and S $1s\rightarrow\sigma^*$ (S–C) peaks (Fig. 2). The Auger decay spectra show that both resonances are mostly followed by the sulfur $KL_{2,3}L_{2,3}$ spectator Auger decay. As discussed in the previous paper, the high desorption yield of Cl^+ ions at the Cl $1s\rightarrow\sigma^*$ resonance in adsorbed $SiCl_4$ (Refs. 4 and 5) is due to the excited electron (spectator electron) in the highly antibonding σ^* orbital. Similarly, the high desorption yields of the CH_3^+ and S^+ ions at the S $1s\rightarrow\sigma^*$ resonances in comparison with those at higher-energy excitation is interpreted in terms of the spectator electrons in the highly antibonding σ^* orbital. The special point in the present case is that the spectator electrons in the σ^* (S–S) and σ^* (S–C) bonds are localized at the respective sites as was confirmed by the two-step linear kinetic-energy dispersion (Fig. 5). Therefore, the spectator electrons localized at the σ^* (S–C) orbital would break the S–C bond, while those localized at the σ^* (S–S) orbital would cut the S–S bond. The cleavage of the S–C bond will mainly produce the CH_3^+ ions (higher charged ions such as CH_3^{2+} were not separated in the present experiment). This is consistent with the experimental result [Fig. 3(c)]. On the other hand, the S–S bond breaking may produce CH_3S^+ ions. However, the intensity of the CH_3S^+ ions at the S $1s\rightarrow\sigma^*$ (S–S) resonance is extremely low, and only CH_3^+ and S^+ ions are observed in comparable intensity [Fig. 3(b)]. Concerning the desorption of molecular ions, we have observed in the previous work that the desorption of the atomic Cl^+ ions from solid CCl_4 is induced by the spectator electron in the σ^* orbital, but the desorption of molecular CCl_3^+ ions is not specially caused by the Cl $1s\rightarrow\sigma^*$ resonance due to the slow movement of such heavier molecular species.[47] This explanation holds for the absence of the CH_3S^+ desorption at the S $1s\rightarrow\sigma^*$ (S–S) resonance. At present we consider that the comparable yields of the CH_3^+ and S^+ ions in mass spectrum is ascribed to the dissociation of the CH_3S^+ in the course of the desorption process.

In conclusion, the site-selective desorption was clearly observed in the light fragment ions from multilayered DMDS around the sulfur *K*-edge photoexcitation. These site-selective photofragmentation is realized in the photon energy range where a sulfur $KL_{2,3}L_{2,3}$ spectator Auger decay happens. The spectator electrons localized at the σ^* (S–S) and σ^* (S–C) orbitals cause the site-selective bond breaking. Such photochemical processes by core-to-valence resonant excitation will shed light on further site-selective fragmentation and desorption not only in adsorbed molecules but also in bulk materials with the popularization of energy-tunable and polarized synchrotron radiation.

V. SUMMARY

We have investigated the fragment-ion desorption from multilayered DMDS around the sulfur *K*-edge photoexcitation, and observed the site-selective desorption of the CH_3^+ and S^+ ions. The main points elucidated in this work are summarized as follows.

(1) The XANES spectrum around the sulfur *K*-edge exhibits the S $1s\rightarrow\sigma^*$ resonance and shape resonance peaks. The shape resonance excitation induces scarcely any ion desorption. Since the shape resonance excitation is completely followed by the sulfur $KL_{2,3}L_{2,3}$ normal Auger decay, the spectator Auger decay and the localization of the spectator electron in the σ^* orbital are essential for the fragment-ion desorption.

(2) The S $1s\rightarrow\sigma^*$ resonance is split into two components corresponding to the excitations from the S $1s$ to the σ^* orbital in S–S and S–C bonds. The S^+ ions are desorbed mainly at the S $1s\rightarrow\sigma^*$(S–S) resonance while the CH_3^+ ions

desorb predominantly at the S $1s \rightarrow \sigma^*$(S–C) excitation.

(3) The Auger decay spectra revealed that the S $1s \rightarrow \sigma^*$ resonance is mostly followed by the sulfur $KL_{2,3}L_{2,3}$ spectator Auger decay. The linear kinetic-energy dispersion of the sulfur $KL_{2,3}L_{2,3}$ spectator Auger peaks with the incident photon energy shows that two kinds of the spectator Auger decays happen. These decays correspond to those after the S $1s \rightarrow \sigma^*$ (S–S) and S $1s \rightarrow \sigma^*$ (S–C) excitations. This means that the excited electrons are localized at the respective bonds (S–S and S–C) in the course of the Auger decay.

(4) Based on (2) and (3), the observed site-selective desorption is interpreted in terms of the localization of the spectator electrons in the respective orbitals, i.e., σ^* (S–S) and σ^* (S–C).

ACKNOWLEDGMENTS

The authors would like to acknowledge the staff of the Photon Factory of the National Laboratory for High Energy Physics for their assistance throughout the experiments. This work was performed under the approval of the Photon Factory Program Advisory Committee (PF-PAC No. 95G410).

[1] R. A. Rosenberg, P. J. Love, P. R. LaRoe, V. Rehn, and C. C. Parks, Phys. Rev. B **31**, 2634 (1985).
[2] R. Treichler, W. Riedl, P. Feulner, and D. Menzel, Surf. Sci. **243**, 239 (1991).
[3] Y. Baba, K. Yoshii and T. A. Sasaki, Surf. Sci. **341**, 190 (1995).
[4] Y. Baba, K. Yoshii, and T. A. Sasaki, Surf. Sci. **357/358**, 302 (1996).
[5] Y. Baba, K. Yoshii, H. Yamamoto, T. A. Sasaki, and W. Wurth, Proceedings of the International Symposium on Material Chemistry in Nuclear Environment, Tsukuba, Japan, 1996, p. 391.
[6] Y. Baba, K. Yoshii, and T. A. Sasaki (unpublished).
[7] D. Coulman, A. Puschmann, U. Höfer, H. P. Steinrück, W. Wurth, P. Feulner, and D. Menzel, J. Chem. Phys. **93**, 58 (1990).
[8] H. Ikeura, T. Sekiguchi, K. Tanaka, K. Obi, N. Ueno, and K. Honma, Jpn. J. Appl. Phys. **32**, 246 (1993).
[9] K. Tanaka, M. C. K. Tinone, H. Ikeura, T. Sekiguchi, and T. Sekitani, Rev. Sci. Instrum. **66**, 1474 (1995).
[10] T. Sekiguchi, H. Ikeura, K. Tanaka, K. Obi, N. Ueno, and K. Honma, J. Chem. Phys. **102**, 1422 (1995).
[11] M. C. K. Tinone, K. Tanaka, J. Maruyama, N. Ueno, M. Imamura, and N. Matsubayashi, J. Chem. Phys. **100**, 5988 (1994).
[12] M. C. K. Tinone, T. Sekitani, K. Tanaka, J. Maruyama, and N. Ueno, Appl. Surf. Sci. **79/80**, 89 (1994).
[13] W. Eberhardt, T. K. Sham, R. Carr, S. Krummacher, M. Strongin, S. L. Weng, and D. Wesner, Phys. Rev. Lett. **50**, 1038 (1983).
[14] K. Müller-Dethlefs, M. Sander, L. A. Chewter, and E. W. Schlag, J. Phys. Chem. **88**, 6098 (1984).
[15] P. Morin, G. G. B. de Souza, I. Nenner, and P. Lablanquie, Phys. Rev. Lett. **56**, 5755 (1986).
[16] J. Murakami, M. C. Nelson, S. L. Anderson, and D. M. Hanson, J. Chem. Phys. **85**, 5755 (1986).
[17] M. C. Nelson, J. Murakami, S. L. Anderson, and D. M. Hanson, J. Chem. Phys. **86**, 4442 (1986).
[18] S. Nagaoka, S. Suzuki, and I. Koyano, Phys. Rev. Lett. **58**, 1524 (1987).
[19] A. P. Hitchcock, P. Lablanquie, P. Morin, E. Lizon, A. Lugrin, M. Simon, P. Thirty, and I. Nenner, Phys. Rev. A **37**, 2448 (1988).
[20] K. Ueda, E. Shigemasa, Y. Sato, S. Nagaoka, I. Koyano, A. Yagishita, T. Nagata, and T. Hayaishi, Chem. Phys. Lett. **154**, 357 (1989).
[21] S. Nagaoka, I. Koyano, K. Ueda, E. Shigemasa, Y. Sato, A. Yagishita, T. Nagata, and T. Hayaishi, Chem. Phys. Lett. **154**, 363 (1989).
[22] S. Nagaoka, J. Ohshita, M. Ishikawa, T. Matsuoka, and I. Koyano, J. Phys. Chem. **97**, 1488 (1993).
[23] N. Saito, J. D. Bozek, and I. H. Suzuki, Chem. Phys. **188**, 367 (1994).
[24] S. Nagaoka, J. Oshita, M. Ishikawa, K. Takano, U. Nagashima, T. Takeuchi, and I. Koyano, J. Chem. Phys. **102**, 6078 (1995).
[25] S. Bodeur and J. M. Esteva, Chem. Phys. **100**, 415 (1985).
[26] C. Dezarnaud, M. Tronc, and A. P. Hitchcock, Chem. Phys. **142**, 455 (1990).
[27] C. Dezarnaud, M. Tronc, and A. Modelli, Chem. Phys. **156**, 129 (1991).
[28] K. Kimura, S. Katsumata, Y. Achiba, T. Yamazaki, and S. Iwata, in *Handbook of He I Photoelectron Spectra of Fundamental Organic Molecules* (Japan, Science Society Press, Tokyo, 1981).
[29] I. Tokue, A. Hiraya, and K. Shobatake, Chem. Phys. **130**, 401 (1989).
[30] S. Bao, C. F. McConville, and D. P. Woodruff, Surf. Sci. **187**, 133 (1987).
[31] A. P. Hitchcock, S. Bodeur, and M. Tronc, Physica B **158**, 257 (1989).
[32] Y. Baba, K. Yoshii, and T. A. Sasaki, Surf. Sci. (in press).
[33] T. A. Sasaki, Y. Baba, H. Yamamoto, and K. Yoshii (unpublished).
[34] M. O. Krause, J. Phys. Chem. Ref. Data **8**, 307 (1979).
[35] T. A. Carlson, P. Gerald, M. O. Krause, G. von Wald, J. W. Taylor, F. A. Grimm, and B. P. Pullen, J. Electron Spectrosc. Relat. Phenom. **47**, 227 (1988).
[36] Y. Baba, T. A. Sasaki, and H. Yamamoto, Phys. Rev. B **49**, 709 (1994).
[37] Y. Baba, H. Yamamoto, and T. A. Sasaki, Surf. Sci. **307**, 896 (1994).
[38] K. Yoshii, Y. Baba, and T. A. Sasaki, J. Surf. Sci. Soc. Jpn. **16**, 453 (1995).
[39] T. A. Sasaki, Y. Baba, K. Yoshii, and H. Yamamoto, J. Phys.: Condens. Matter **7**, 4385 (1995).
[40] T. A. Sasaki, Y. Baba, K. Yoshii, and H. Yamamoto, J. Electron Spectrosc. Relat. Phenom. **76**, 411 (1995).
[41] K. Yoshii, Y. Baba, and T. A. Sasaki, J. Electron Spectrosc. Relat. Phenom. **79**, 215 (1996).
[42] M. L. Knotek and P. J. Feibelman, Phys. Rev. Lett. **40**, 964 (1978).
[43] D. Menzel, Nucl. Instrum. Meth. Phys. Res. B **13**, 507 (1986).
[44] G. Rocker, P. Feulner, R. Scheuerer, L. Zhu, and D. Menzel, Phys. Scr. **41**, 1014 (1990).
[45] D. Menzel, Appl. Phys. A **51**, 163 (1990).
[46] D. Menzel, G. Rocker, H. P. Steinrück, D. Coulman, P. A. Heimann, W. Huber, P. Zebisch, and D. R. Lloyd, J. Chem. Phys. **96**, 1724 (1992).
[47] Y. Baba, K. Yoshii, and T. A. Sasaki (unpublished).